Electronic Supplementary Information

Establishment of a universal and sensitive plasmonic biosensor platform based on the hybridization chain reaction (HCR) amplification induced by a triple-helix molecular switch

Ganglin Wang,[a] Jingfeng Li, [b] Yong He, [c] Jun Liu, [d] Mingxia Yu[e] and Guoping Wang*[a]

a. Hubei Bioinformatics & Molecular Imaging Key Laboratory, Department of Biomedical Engineering, College of Life Science and Technology, Huazhong University of Science and Technology, Wuhan 430074, P. R. China. E-mail: wangguoping@hust.edu.cn.

b. Department of Orthopedics, Zhongnan Hospital of Wuhan University, Wuhan 430071, P. R. China.

c. Department of Nuclear Medicine and PET Center, Zhongnan Hospital of Wuhan University, Wuhan 430071, P. R. China.

d. School of Power and Mechanical Engineering, Wuhan University, Wuhan 430071, P. R. China.

e. Department of Clinical Laboratory, Zhongnan Hospital of Wuhan University, Wuhan 430071, P. R. China.

*Corresponding author. Tel & Fax: 862787792072;
E-mail: *wangguoping@hust.edu.cn.*

Table S1. DNA sequences used in this study

Name	Sequence (5′ to 3′)
UT	AGAGAGAGAGAGGGAAAGAGAGAGACACACAC AC
M1	CTCTCTCTTTCCCTCTCTCTCTCTCGGCAGAGAGA GAGAGGGAAAG TTTTTTTTTTTTTTT
M2	AGAGAGAGAGAGGGAAAGAGAGAGCTTTCCCTC TCTCTCTCTGCCG TTTTTTTTTTTTTTT
P1 for miRNA detection	CTCCCTTT*TCAACATCAGTCTGATAAGCTA*ATTTCCCT C
P2 for ATP detection	CTCCCTTT*ACCTGGGGGAGTATTGCGGAGGAAGG*T TTTCCCTC
P3 for thrombin detection	TCCCTTT *GGTTGGTGTGGTTGG* TTTCCCT
miRNA-21(DNA sequence)	TAGCTTAUCAGACTGATGTTGA
MiRNA-141 (DNA sequence)	TAACACTGTCTGGTAAAGATGG
MiRNA-155 (DNA sequence)	TTA ATG CTA ATC GTG ATA GGG GT
SH-DNA for DNA-AuNPs probes	SH-$(CH_2)_6$ -AAAAAAAAAAAAAAA

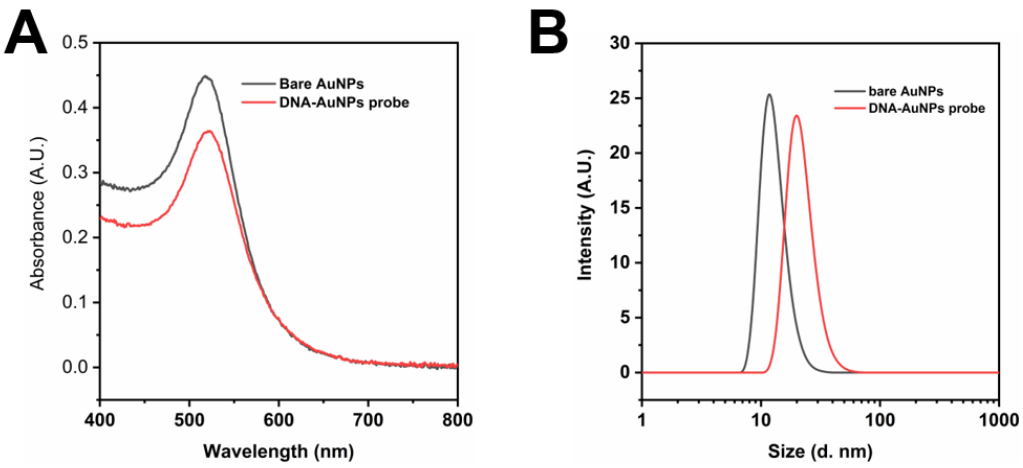

Fig. S1 UV-visible absorption spectrum (A) and dynamic Light Scattering (B) of AuNPs (black line) and DNA-AuNPs probes (red line).

Characterization of P1 and UT THMS complex assembly and disassembly

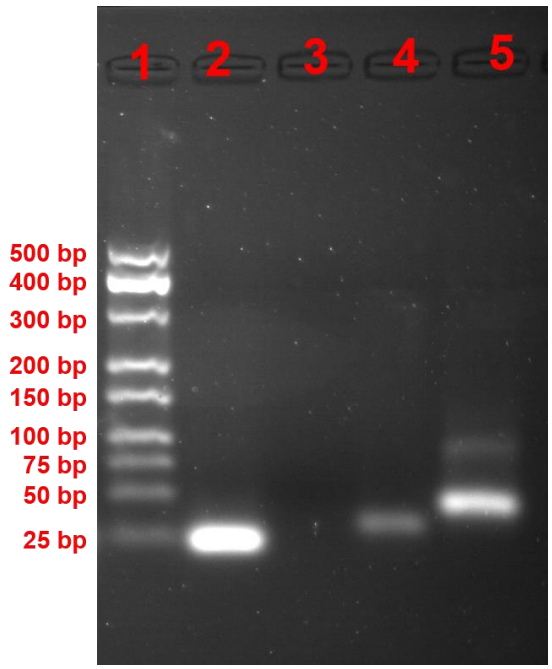

Fig. S2 3.5% agarose gel electrophoresis demonstrates P1 and UT THMS complex assembly and disassembly: lane 1: 25~500 bp ladder markers；lane 2:1.0 μM P1; lane 3: 1.0 μM UT; lanes 4: 1.0 μM P1+1.0 μM UT; lanes 5, 1.0 μM P1+1.0 μM UT+0.5 μM miRNA-21;

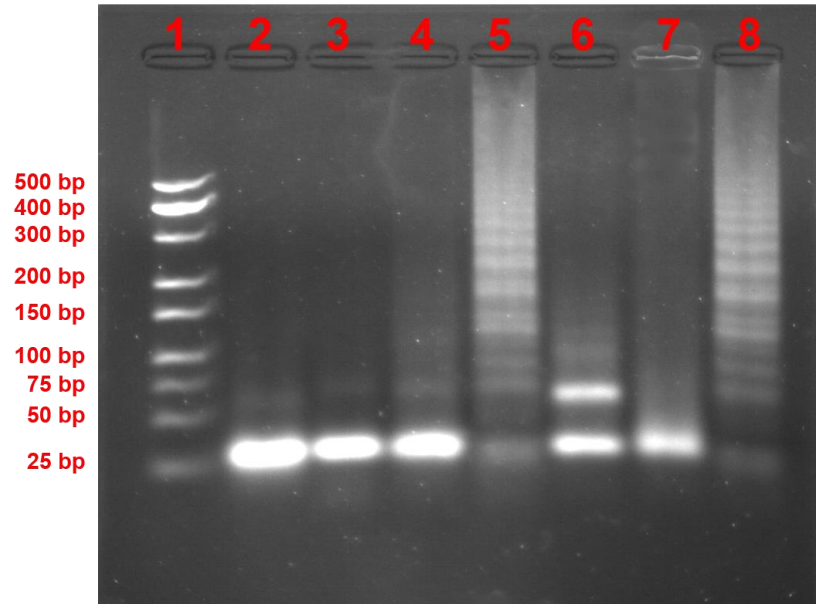

Fig. S3 3.5% agarose gel electrophoresis demonstrates HCR products in miRNA-21 system. Lane 1: the DNA marker; Lane 2: M1(1μM); Lane 3: M2(1μM); Lane 4: M1(1μM) + M2(1μM); Lane 5: M1(1μM) + M2(1μM) + UT (0.2 μM); Lane 6: M1(1μM) + M2(1μM) + miRNA-21(0.2 μM); Lane 7: M1(1μM) + M2(1μM) + P1-UT THMS(0.2 μM); Lane 8: M1(1μM) + M2(1μM) +P1-UT THMS(0.2 μM) + miRNA-21(0.2 μM).

Characterization of P2 and UT THMS complex assembly and disassembly

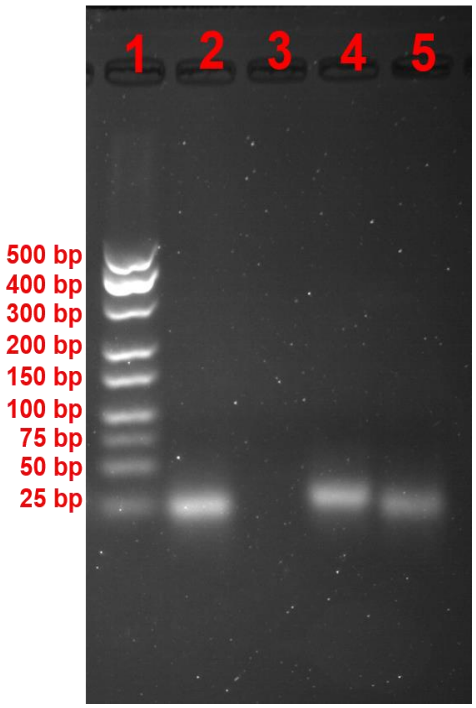

Fig. S4 3.5% agarose gel electrophoresis demonstrates P2 and UT THMS complex assembly and disassembly: lane 1: 25~500 bp ladder markers；lane 2:1.0 μM P2; lane 3: 1.0 μM UT; lanes 4: 1.0 μM P2+1.0 μM UT; lanes 5, 1.0 μM P2+1.0 μM UT+0.5 μM ATP;

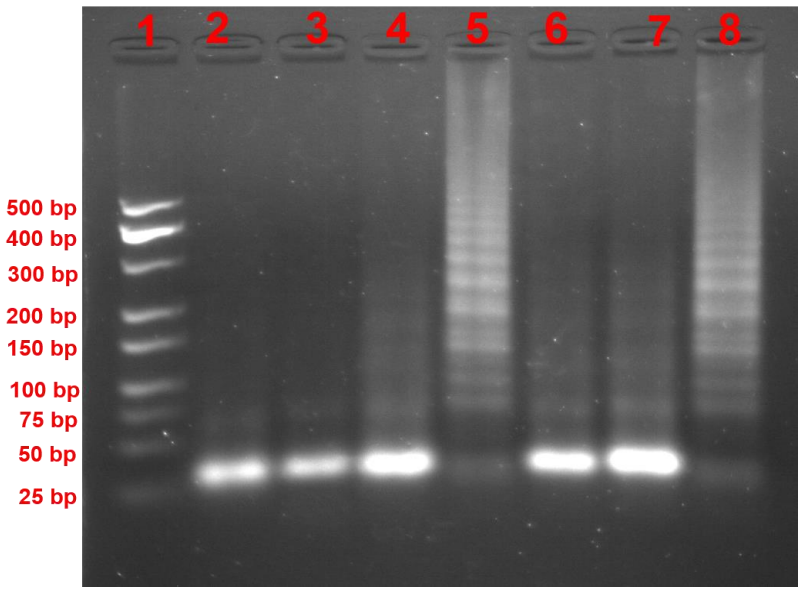

Fig. S5 3.5% agarose gel electrophoresis demonstrates HCR products in miRNA-21 system. Lane 1: the DNA marker; Lane 2: M1(1μM); Lane 3: M2(1μM); Lane 4: M1(1μM) + M2(1μM); Lane 5: M1(1μM) + M2(1μM) + UT (0.2 μM); Lane 6: M1(1μM) + M2(1μM) +ATP(1 μM); Lane 7: M1(1μM) + M2(1μM) + P2-UT THMS(0.2 μM); Lane 8: M1(1μM) + M2(1μM) +P2-UT THMS(0.2 μM) + ATP(1 μM).

Characterization of P3 and UT THMS complex assembly and disassembly

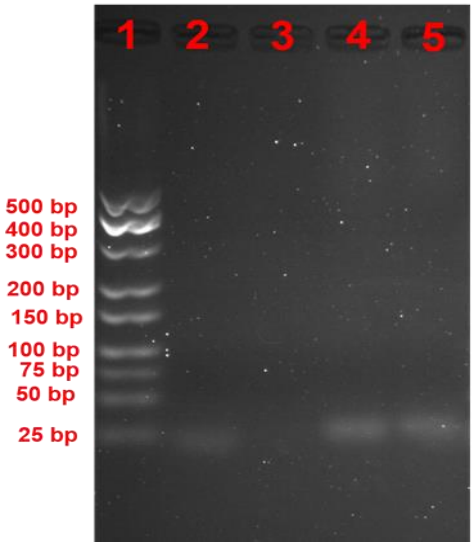

Fig. S6 3.5% agarose gel electrophoresis demonstrates P3 and UT THMS complex assembly and disassembly: lane 1: 25~500 bp ladder markers；lane 2:1.0 μM P3; lane 3: 1.0 μM UT; lanes 4: 1.0 μM P3+1.0 μM UT; lanes 5, 1.0 μM P3+1.0 μM UT+0.5 μM Tmb.

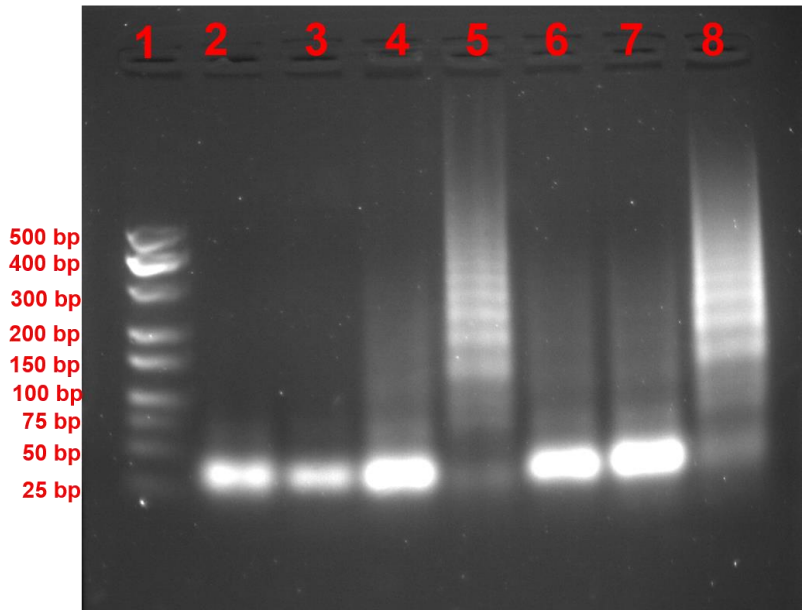

Fig. S7 3.5% agarose gel electrophoresis demonstrates HCR products in Tmb. Lane 1: the DNA marker; Lane 2: M1(1μM); Lane 3: M2(1μM); Lane 4: M1(1μM) + M2(1μM); Lane 5: M1(1μM) + M2(1μM) + UT (0.2 μM); Lane 6: M1(1μM) + M2(1μM) + miRNA-21(0.2 μM); Lane 7: M1(1μM) + M2(1μM) + P3-UT THMS(0.2 μM); Lane 8: M1(1μM) + M2(1μM) +P3-UT THMS(0.2 μM) + Tmb(0.2 μM).

Optimization of detection conditions

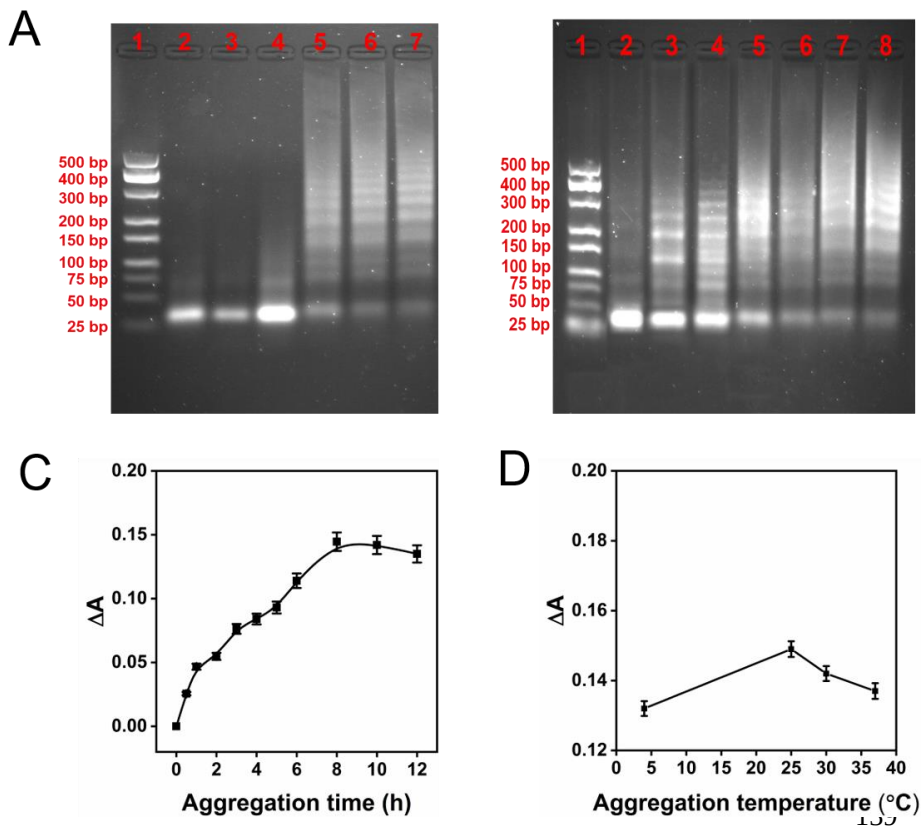

Fig. S8 Effects of (A) the HCR temperature, lane 1: the DNA marker; Lane 2: M1(1μM); Lane 3: M2(1μM); Lane 4: M1(1μM) + M2(1μM); Lane 5: M1(1μM) + M2(1μM) + UT (0.2 μM) 4 ℃ for 2 h; Lane 6: M1(1μM) + M2(1μM) + UT (0.2 μM) 25 ℃ for 2 h; Lane 7: M1(1μM) + M2(1μM) + UT (0.2 μM) 37 ℃ for 2 h; (B) the HCR time, lane 1: the DNA marker; Lane 2: M1(1μM) + M2(1μM) + UT (0.2 μM) 0 min at 37 ℃; Lane 3: M1(1μM) + M2(1μM) + UT (0.2 μM) for 30 min at 37 ℃; Lane 4: M1(1μM) + M2(1μM) + UT (0.2 μM) for 1h at 37 ℃; Lane 5: M1(1μM) + M2(1μM) + UT (0.2 μM) 1.5 min at 37 ℃; Lane 6: M1(1μM) + M2(1μM) + UT (0.2 μM) 2h at 37 ℃; Lane 7: M1(1μM) + M2(1μM) + UT (0.2 μM) 4h at 37 ℃; Lane 8: M1(1μM) + M2(1μM) + UT (0.2 μM) 8h at 37 ℃; (C) and (D)Effects of DNA-AuNPs probes and HCR products aggregation time and temperature. The error bars represent the standard deviations of three replicates.

Calculation of limit of detection (LOD)

Limit of detection was calculated using the following formula (*Anal. Chem.*, 2012, **84**, 2837−2842, *Biosens. Bioelectron.*, 2015, **63**, 311–316.):

$$LOD = 3\sigma/s;$$

where σ is the standard deviation of the response and s is the slope of the calibration curve of the analyte.

For example, the calculation of the LOD for miRNA was shown here:

The linear equation was expressed as $y=0.01571+3.4452\times10^{-4}x$, which was obtained from Fig.4C in the manuscript, so we can know the $s=3.4452\times10^{-4}$. The standard deviation of the response was σ=0.002298, which was obtained from the standard deviation of signal of the blank sample. Then, the LOD was calculated as follows: $LOD=3\sigma/s=3\times0.002298/3.4452\times10^{-4}\approx 20$ pM.

Similarly, we can use the same method to calculate the LOD of ATP and thrombin.

Table S2 Comparison of the proposed method with other methods for miRNA detection

Detection Method	Linear range	Limit of detection	Reference
Fluorescent	1−50 nM	330 pM	*Anal. Methods*, 2016, **8**, 8492-8497
Electrochemical	0.2−755 nM	100 pM	*Bioelectrochemistry*, 2017, **116**, 17-23.
Plasmonic biosensor	10 nM−20 μM.	300 pM	*ACS Appl. Mater. Interfaces*, 2015, **7**, 2459-2466.
Fluorescence resonance energy transfer	0.1−200 nM	100 pM	*ACS Appl. Mater. Interfaces*, 2015, **7**, 16152−16156.
Surface plasmon resonance	0.02−10 pM	45 pM	*Microchim. Acta*, 2017, **184,** 2637-2644.
Plasmonic biosensor-HCR	20−200 pM	20 pM	Our work

Table S3 Comparison of the proposed method with other methods for ATP detection

Detection Method	Linear range	Limit of detection	Reference
Fluorescence Polarization Strategy	0.067−26.7 μM	34.4 nM	*Anal. Chem.* 2018, **90**, 13708−13713.
Electrochemical	1 nM−100 μM	21.33 ± 4.1 nM	*Anal. Chem.* 2018, **90**, 4968−4971
Fluorescence resonance energy transfer	0.03−2 mM	0.03 mM	*Anal. Chem.* 2017, **89**, 10941−10947
Surface plasmon resonance	12.4 pM−2.0 nM	12.4 pM	*Anal. Chem.* 2012, **84**, 2837−2842
Plasmonic biosensor-HCR	20−500 nM	15.6 nM	Our work

Table S4 Comparison of the proposed method with other methods for thrombin detection

Detection Method	Linear range	Limit of detection	Reference
Fluorescent	62.5−187.5 pM	31.3 pM pM	*Anal. Chem.* 2010, **82,** 2341–2346.
Electrochemical	10 pM−50 nM	5.6 pM	*Anal. Chem.* 2016, **88,** 8218−8223.
Colorimetric biosensor	0.1−15 nM	0.1 nM	*ACS Appl. Mater. Interfaces* 2016, **8**, 102−108.
Paper analytical device	0−2 μM	16 nM	*Anal. Chem.* 2014, **86,** 6166−6170.
Plasmonic biosensor-HCR	20−800 pM	18.4 pM	Our work